COBEM 99
XV Congresso Brasileiro de Engenharia Mecânica
15th Brazilian Congress of Mechanical Engineering
22 - 26 de Novembro de 1999 / November 22 - 26, 1999 Águas de Lindóia, São Paulo,

DEVELOPMENT OF A BEARING AND POWER TRANSFER ASSEMBLY MECHANISM FOR SMALL SATELLITES

Mário C. Ricci
Sebastião E. C. Varotto
National Institute for Space Research, Space Mechanics and Control Division
Cx. P. 515 – 12201-970 – São José dos Campos, SP, Brasil

Abstract. *This work intends to show some aspects about the mechanical layout and modeling of a BAPTA (Bearing and Power Transfer Assembly) mechanism in development involving a government institution (INPE) and private companies. The design here described is being evolved for application in small satellites (~0.5 kW with a rigid solar panel of ~1.0 kgm^2). The selected concept uses a conventional 1.8^o stepper motor and a 100:1 harmonic drive reduction gearing to achieve a theoretical output step size of 0.018^o. Simulations in computer are showing that significant interaction with the solar array and spacecraft can be avoided (spacecraft pitch disturbing velocity is lower than 10^{-3} deg/sec) with power consumption as low as 3 to 5 W. The adequate determination of the power consumption is possible due to a adequate representation of magnetic non-linearity in the motor, including its effect on electromagnetic torque production. The reliable prediction of the important dynamic characteristics of the motor and general system necessitates a precise representation of the flux-linkage data. A good example is the single-step damping, which can be predicted satisfactorily only if the current disturbance and associated power loss in each stator circuit are calculated correctly. This requires that the rate of change of flux-linkage be defined accurately for any combination of the system variables.*

Keywords: *BAPTA, Small Satellites, Modeling*

1. INTRODUCTION

Some kinds of artificial satellites must be appointed toward the Earth while the solar panels must be appointed toward the Sun in order of maximize the solar energy that reaches the solar panels. These kinds of satellites shall incorporate a BAPTA (Bearing and Power Transfer Assembly) mechanism.

The BAPTA is a Power Subsystem mechanism that performs the tasks of maintain the one degree-of-freedom of the output axis (panel axis) while transmits the electrical and

power signals from the panel to the satellite body. The BAPTA consists basically of three main units: a) the Bearing Unit, b) the Drive Unit and c) the Slip Rings Unit.

The design here described is being evolved for application in small satellites with a rigid solar panel of about 0.5 kW and 1.0 kgm^2 of inertia. The platform inertia shall be not less than 20 kgm^2.

In this work we concentrate the efforts in the modeling of the Drive Unit. Two solutions were considered for the Drive Unit: a) closed-loop synchronous system and b) open-loop incremental motion control system. Since the orbital period is too large (on the order of 10^2 min) the nominal speed and its variation are very low and very difficult to measuring. Therefore, the second solution is to be the better choice and the selected concept uses a conventional 1.8^o stepper motor and a 100:1 harmonic drive reduction gearing to achieve a theoretical output step size of 0.018^o (Fig. 1).

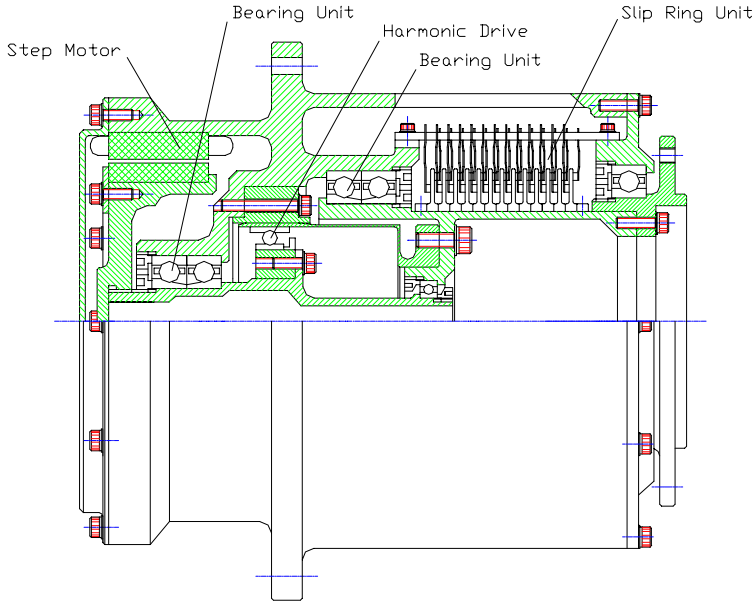

Figure 1- BAPTA mechanism for small satellite.

In normal mode the mechanism operates in open loop with a frequency of about 3.21 steps per second. When the solar panel's normal deviates from Satellite-Sun vector of an angle greater than two degrees a signal is send to the control electronics to modify the system's clock in order to maintain the solar panel's pointing requirements.

The main specifications for the BAPTA mechanism, operating in a satellite with an orbital period of 107 minutes, are given in Table 1.

Table 1. Main specifications for the BAPTA mechanism

Orbital mean rate (orbital period of 107 min)	0.056 ^{o}/s	Total mass	< 2 kg
		Power	5 W
Pitch disturbing velocity	< 10^{-3} ^{o}/s	Overall dimensions	
Solar panel's inertia	1 kg m^2	Electronic	120x120x120 mm
Platform inertia	20 kg m^2	Mechanical	120x120x120 mm

2. EQUATIONS OF MOTION

The system under investigation consists of a rigid asymmetric platform (with inertia J_1, attitude θ_1 and angular velocity ω_1) linked to an axisymmetric body (with inertia J_2, attitude θ_2 and angular velocity ω_2), stands for the motor's rotor and reduction gearing, that is connected by a lossy torsional spring to a third axisymmetric body (with inertia J_3, attitude θ_3 and angular velocity ω_3), representing the rigid solar panel and the yoke as illustrated in Fig. 2.

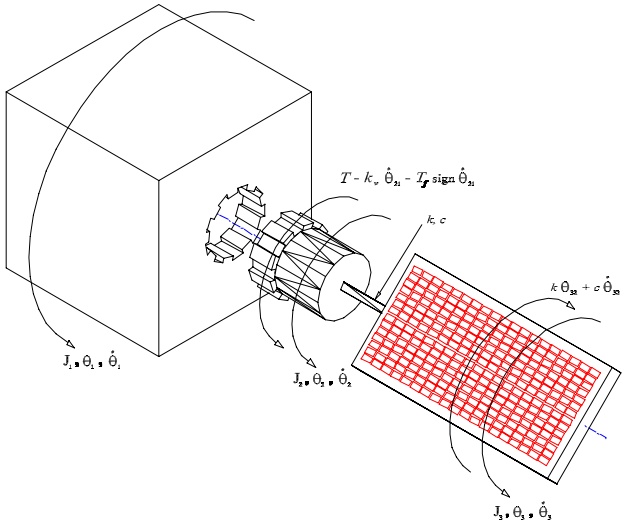

Figure 2- A simplified model for a small satellite with a rigid solar panel.

Disregarding the translational motion of the spacecraft the degrees-of-freedom of the system are θ_1, θ_2 and θ_3, where the attitude θ_1 is to be controlled with respect to an absolute reference and the masses are free to oscillate about the common axis of symmetry. The equations of motion may be arranged into eight 1st-order differential equations:

$$\frac{d\theta_1}{dt} = \omega_1, \tag{1}$$

$$\frac{d\omega_1}{dt} = -\frac{1}{J_1}\left[T(i_{AC},\theta_{21}) + T(i_{BD},\theta_{21}) - k_v\omega_{21} - T_f\frac{\omega_{21}}{|\omega_{21}|}\right], \tag{2}$$

$$\frac{d\theta_2}{dt} = \omega_2, \tag{3}$$

$$\frac{d\omega_2}{dt} = \frac{10^4}{J_2}\left[T(i_{AC},\theta_{21}) + T(i_{BD},\theta_{21}) - k_v\omega_{21} - T_f\,\frac{\omega_{21}}{|\omega_{21}|}\right] + \frac{1}{J_2}\left(k\theta_{32} + c\omega_{32}\right), \tag{4}$$

$$\frac{d\omega_3}{dt} = -\frac{1}{J_3}\left[k\theta_{32} + c\omega_{32}\right], \tag{5}$$

$$\frac{d\theta_3}{dt} = \omega_3, \tag{6}$$

$$\frac{di_{AC}}{dt} = \frac{1}{\dfrac{\partial\lambda_A}{\partial i_{AC}}}\left[\frac{V_A - V_C}{2} - \frac{Ri_{AC}}{2} - \omega_{21}\frac{\partial\lambda_A}{\partial\theta_{21}}\right], \tag{7}$$

$$\frac{di_{BD}}{dt} = \frac{1}{\dfrac{\partial\lambda_B}{\partial i_{BD}}}\left[\frac{V_B - V_D}{2} - \frac{Ri_{BD}}{2} - \omega_{21}\frac{\partial\lambda_B}{\partial\theta_{21}}\right], \tag{8}$$

where Eqs. (1) and (2) are the equations for satellite body; Eqs. (3) and (4) are representing the rotor axis and reduction gearing; Eqs. (5) and (6) refers to the solar panel plus yoke and Eqs. (7) and (8) are the electromagnetic equations for motor currents.

The symbols in the Eqs. (1-8) are the following: c is the equivalent damping coefficient; k is the spring constant; k_v is the coefficient of viscous friction; T_f is the friction torque; T is the electromagnetic torque; i_{AC} and i_{BD} are the net motor currents; R is the total series resistance of a stator circuit; V_A, V_B, V_C and V_D are the phase voltages; $\theta_{ij} \equiv \theta_i - \theta_j$; $\omega_{ij} \equiv \omega_i - \omega_j$; λ_A and λ_B are the flux-linkages and *t* is the time.

3. MOTOR'S MODEL

3.1 General Considerations

The motor under consideration here is a low-speed, two-phase synchronous inductor motor as described by Snowdon and Madsen (1962) provided with bifilar windings arrangement. A translated version to Portuguese can be found in Ricci (1986).

With bifilar windings the motor can be thought as a four phase machine and these will be referred to as A, B, C and D respectively. Phases A and C are the two components of one bifilar winding and phases B and D are the two components of the other bifilar winding. With this arrangement, 100% coupling exists between two phases comprising a bifilar pair and currents of the same polarity flowing in the phases A and C, for instance, produce opposing magnetization of the core. Because the quadrature between the two bifilar windings the mutual coupling between them can be considered negligible.

Taking phase A, for example, the flux-linkage λ_A may be expressed in terms of net coil current, $i_{AC} \equiv i_A - i_C$, and the angular position of the rotor θ, i.e., $\lambda_A(i_{AC}, \theta)$, and will be determined by fitting mathematical functions to experimental flux-linkage data obtained from static tests.

The flux-linkage can be expressed analytically as

$$\lambda_A(i_{AC}, \theta) = \lambda_{PMA}(\theta) + \lambda_a(i_{AC}, \theta), \tag{9}$$

with $\lambda_{PMA}(\theta)$ being a flux-linkage of phase A due to the permanent magnet flux when the net current in bifilar pair A-C is zero, and $\lambda_a(i_{AC}, \theta)$ representing the change in flux linkage of phase A which occurs owing to the flow of a net current i_{AC} in the coils of that phase.

The electromagnetic torque $T(i_{AC}, \theta)$ can be calculated from the magnetic co-energy to obtain (Pickup and Russel (1980))

$$T(i_{AC}, \theta) = i_{AC} \frac{d\lambda_{PMA}(\theta)}{d\theta} + \frac{\partial}{\partial \theta} \int_0^{i_{AC}} \lambda_a(i'_{AC}, \theta) di'_{AC}. \tag{10}$$

Thus, the torque consists of two components. The first term of Eq. (10), can be thought of loosely as the torque produced by the interaction of the permanent magnet flux and the coil current i_{AC}. Similarly, the second term, may be considered to result from the interaction of the current-dependent flux-linkage and the coil current.

A similar $\lambda_B(i_{BD}, \theta)$ exists, of course, appropriate to the bifilar-pair B-D.

3.2 Mathematical Representation of Flux-linkage

3.2.1 Permanent Magnet Flux-linkage

The flux-linkage of phase A from the permanent magnet is symmetrical about the stable zero-torque position $(N_r\theta = 0^\circ)$ and the unstable zero-torque position $(N_r\theta = 180^\circ)$, and is equal and opposit about $N_r\theta = 90^\circ$, with N_r being the number of rotor teeth. Thus, the following function fitting is suitable for $\lambda_{PMA}(\theta)$, in according to Pickup and Russel (1980),

$$\lambda_{PMA}(\theta) = \lambda_1 \cos(N_r\theta) + \lambda_3 \cos 3(N_r\theta), \tag{11}$$

where the coefficients are $\lambda_1 = 7.45 \times 10^{-3}$ Vs and $\lambda_3 = 5.14 \times 10^{-5}$ Vs. The Figure 3(a) shows the experimental measurements and theoretical representation from curve fit for the permanent magnet flux-linkage.

3.2.2 Current-dependent Flux-linkage

The current-dependent linkage of phase A can be measured by using the bifilar-wound coils of phase C as a closely-coupled search coil connected to a fluxmeter. Because of the equal number of turns on phases A and C this arrangement gives a direct reading of the flux-linkage changes which occur in phase A.

A good aproximation for the flux-linkage is achieved by (Pickup and Russel , 1980)

$$\lambda_a(i_{AC},\theta)=\sum_{r=0}^{2}\left(B_{1r}i_{AC}+B_{3r}i_{AC}^3+B_{jr}i_{AC}^5\right)\cos r\left(N_r\theta\right), \tag{12}$$

where the coefficients, obtained by the least-square method, are shown in Table 2. The Figure 3(b) shows the current-dependent flux-linkage fitting as a function of angular position.

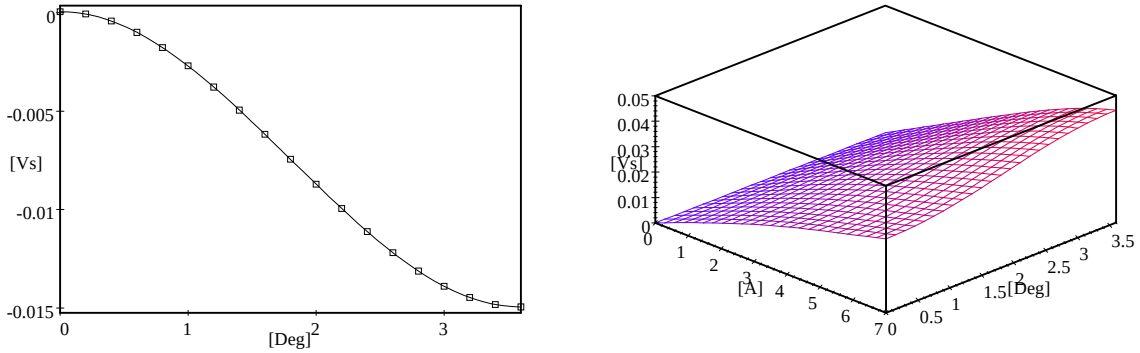

(a) (b)

Figure 3- (a) Permanent magnet flux-linkage. Experimental and theoretical values; (b) Current-dependent flux-linkage fitting.

Table 2. Current-dependent flux-linkage fitting coefficients

r	$B_{1r}\times10^{-3}$	$B_{3r}\times10^{-5}$	$B_{5r}\times10^{-7}$
0	6.234470	-2.49055	0.858076
1	-0.917669	-1.94243	3.29916
2	-0.170484	0.925831	-1.10692

3.3 Static Torque/Angle Characteristics

In order to solve the simultaneous dynamics equations (1-8), the electromagnetic torque of the machine is required in terms of instantaneous values of the coil currents and

angular position of the rotor. This can be calculated from the flux-linkage. With the functions $\lambda_{PMA}(\theta)$ and $\lambda_a(i_{AC},\theta)$ derived previously, the torque expression for a single phase becomes

$$T(i_{AC},\theta) = -N_r\{i_{AC}[\lambda_1 \sin(N_r\theta) + 3\lambda_3 \sin 3(N_r\theta)] + \sum_{r=1}^{2} r\left(B_{1r}\frac{i_{AC}^2}{2} + B_{3r}\frac{i_{AC}^4}{4} + B_{5r}\frac{i_{AC}^6}{6}\right)\sin r(N_r\theta)\}. \qquad (13)$$

Thus, the two torque components calculated from equation (10) can be evaluated to yield the static torque/angle characteristics at various levels of stator excitation.

4. NUMERICAL RESULTS

Some preliminary results are shown in this section. Since it is the qualitative behaviour of solutions that is of interest, the results are presented here in graphical form. The computations were performed using software for simulating dynamic systems named SIMULINK™ that is an extension to MATLAB™. SIMULINK works with windows called *block diagram*. In these windows the model is created and edited by mouse commands. After definition of the model it can be analysed by simulation algorithms and the progress of the simulation can be viewed while the simulation is running. The results can be made available in the MATLAB workspace when the simulation is complete.

The results of simulation are shown in Figures 4 to 7 and are appropriate to 2-phase-on excitation using the following system's parameters and the switching sequence indicated in Table 3.

Table 3. System's parameters and Sequence of excitation for hybrid motor

J_1	20.0 Kgm^2
J_2	0.01 Kgm^2
J_3	0.8 Kgm^2
k	125.0 Nm/rd
c	0.001 Nms/rd
T_f	0.05 Nm
k_v	0.0005 Nms/rd
V	30 V
R	200 Ω

Step	Phase			
	A	B	C	D
1	On	On	Off	Off
2	On	Off	Off	On
3	Off	Off	On	On
4	Off	On	On	Off

Figures 4(a) and 4(b) show the platform angular velocity. It can see that the spacecraft pitch disturbing velocity is on order of 10^{-5} deg/sec.

Figures 5(a) and 5(b) show the net current i_{AC}. The same magnitude inverted profile it was found to i_{BD}. Figure 6(a) shows the driver's power consumption estimate in watts/phase. It is possible to decrease these values by a factor of three (and even more) by increasing R or switching off the motor current after the settling time has been achieved. The use of the model can be extended to study the effects of using dual-voltage supplies or chopped excitation too.

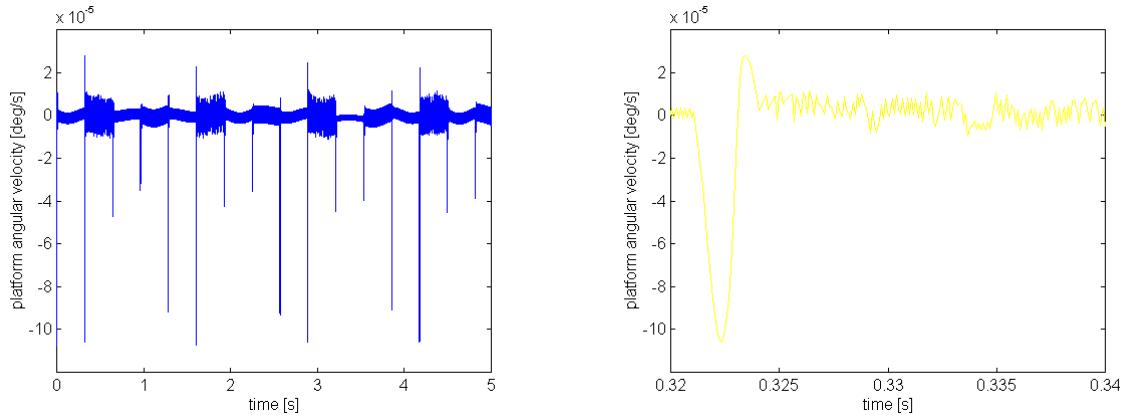

(a) (b)

Fig. 4- Spacecraft pitch disturbing velocity.

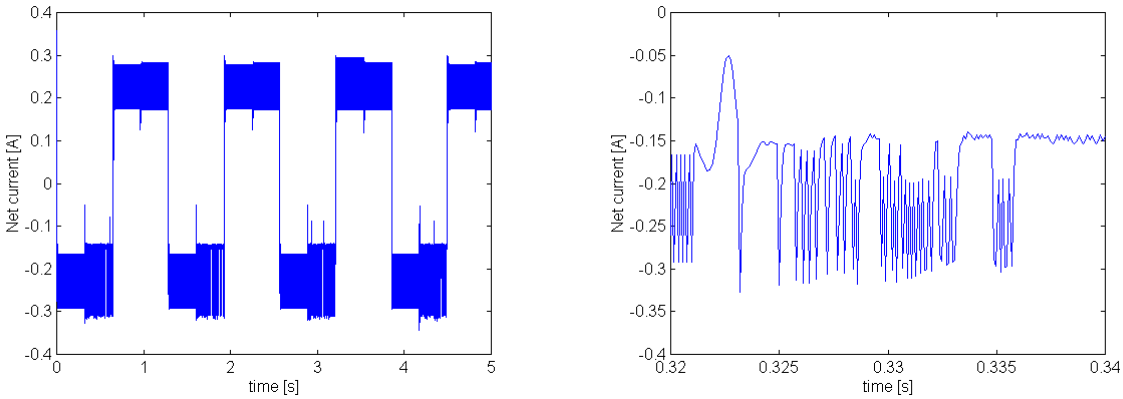

(a) (b)

Fig. 5- Net current i_{AC}.

Figure 6(b) shows the motor torque $T(i_{AC},\theta)$. The same inverted profile it was found to $T(i_{BD},\theta)$. It can observe an average motor torque of about 0.06 Nm under normal operation.

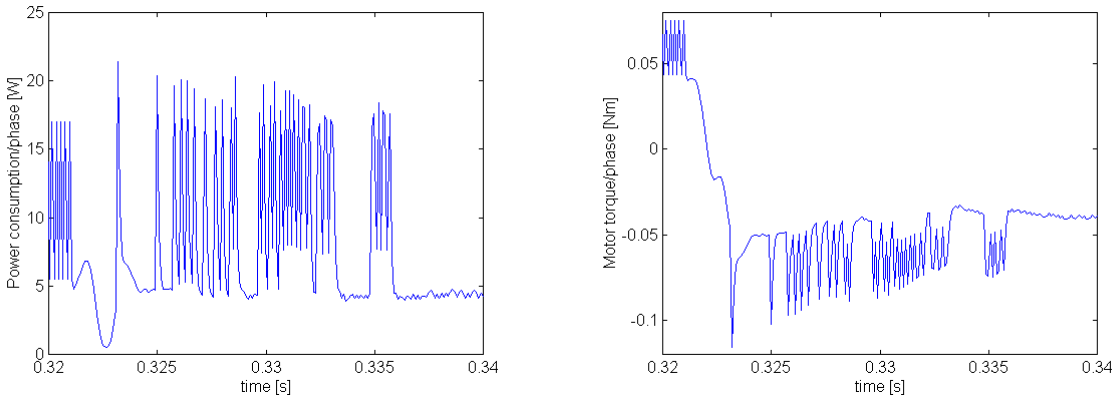

(a) (b)

Fig. 6- (a) Power consumption/phase. (b) Motor torque $T(i_{AC},\theta)$.

Finally. Figures 7(a) and 7(b) show the relative motor's rotor and solar array angular displacements as having the spacecraft as a reference.

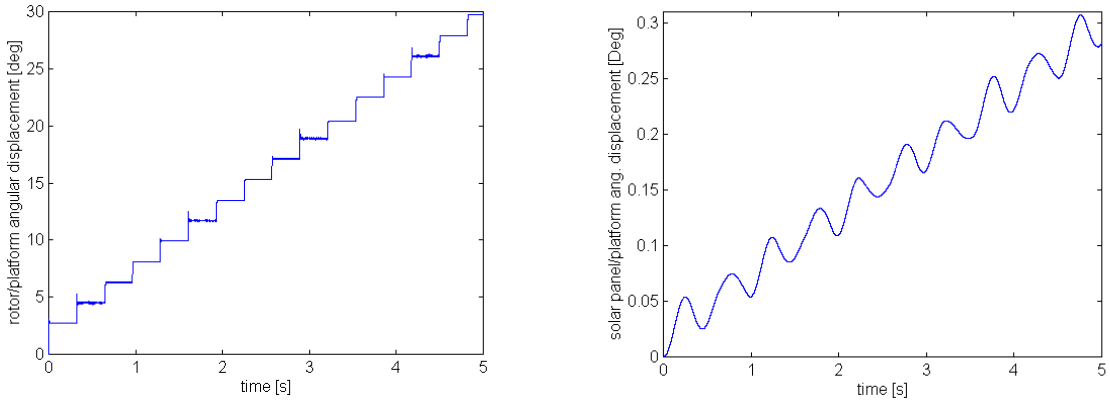

(a) (b)

Fig. 7- (a) Motor's rotor/platform angular displacement. (b) Solar panel/platform angular displacement.

5. CONCLUDING REMARKS

A development model to simulate the interaction between a Bearing and Power Transfer Assembly (BAPTA), conceived to small satellites, and the attitude of a hypothetical satellite with an extendible solar panel has been shown, where has been applied a method for predicting dynamics characteristics for stepper motors developed by Pickup and Russel[3]. This model was used because it considers an important feature of all practical stepping motors applications, that is the non-linearity of the magnetic circuit. For achieve this goal a analytical mathematical function for the flux-linkage of the stator coils, in terms of the coil current and the angular position, was derived and is essential to enable

the system response in the absence of core eddy currents. The system consists of three bodies representing the satellite, the motor's rotor/reduction gearing, and the rigid solar panel/yoke, respectively. The equations may be arranged into eight 1st-order differential equations (six for the bodies and two for the electromagnetic motor currents) and were integrated using the software SIMULINK™. Preliminary results, in normal operation mode, has been shown a low interference between the solar array and spacecraft, with pitch disturbing velocity of 10^{-5} deg/sec and power consumption of 5 W/phase. As we said, it is possible to decrease these values by increasing R or switching off the motor current after the settling time has been achieved. The use of the model can be extended to study the effects of using dual-voltage supplies or chopped excitation too.

Acknowledgment

The authors are grateful to the COBEM'99 Organizing Committee for the invitation to present this work at the 15th Brazilian Congress of Mechanical Engineering to be held in Águas de Lindóia. We wish to thank also the financial support provided by the State of São Paulo Foundation for Research Support (FAPESP).

REFERENCES

Snowdon, A. E.; Madsen, E. W. Characteristics of a Synchronous Inductor Motor. *Trans. Amer. Inst. Elect. Engrs.*, 1962, IGA-81, pp. 1-5.

Ricci, M. C. Motor Síncrono de Indução: Características Construtivas e Operacionais. São José dos Campos, INPE, ago. 1986, 42 p. (INPE-3976-RPE/517).

Pickup, I. E. D.; Russel A. P. A Model for Predicting the Dynamic Characteristics of Hybrid (Permanent Magnet) Synchronous/Stepping Motors. *Proceedings of 9th Annual Symposium on Incremental Motion Control Systems and Devices*, University of Illinois, 1980, pp. 1-13.

SIMULINK A Program for Simulating Dynamic Systems. *User's Guide*, The MathWorks, Inc.

MATLAB *User's Guide*, The MathWorks, Inc.